

Grid Expansion: a Rhombiclike $[L_4Fe_2(Ag_2)_2]$ Complex Containing Ag_2 Dumbbells at Two Vertices

Benjamin Schneider, Serhiy Demeshko, Sebastian Dechert, and Franc Meyer*

Institute of Inorganic Chemistry, Georg-August-University Göttingen, Tammannstraße 4, D-37077 Göttingen, Germany

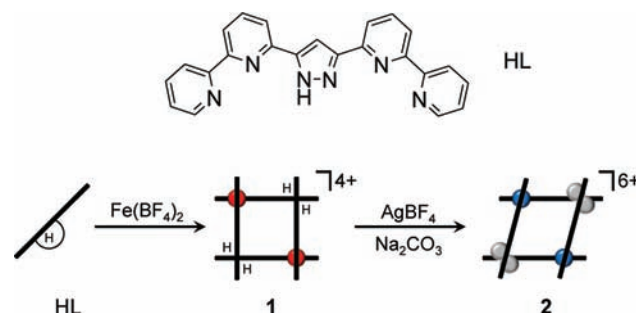
S Supporting Information

ABSTRACT: The pyrazolate-based ditopic ligand HL forms a strongly hydrogen-bonded corner complex dimer $[Fe^{II}(HL)_2](BF_4)_2$ (**1**) with a $[2 \times 2]$ gridlike arrangement of four ligand strands. The two empty vertices can then be filled with $\{Ag_2\}^{2+}$ dumbbells, yielding the unprecedented diferric complex $[L_4Fe^{III}_2(Ag_2)_2](BF_4)_6$ (**2**) that features a rhombiclike structure with an almost planar hexagon of metal ions.

Multinuclear grid-type metal complexes, in which perpendicular ligand strands containing n binding pockets form 2D $[n \times n]$ metalloarrays composed of $2n$ ligands and n^2 metal ions, have gained immense popularity during the past decade.¹ This is not only because grid complexes are aesthetically attractive molecular architectures but also because switchable grids might become components of future information storage and processing devices.² While most of the known grids are homometallic and squarelike, elaborate strategies for the toposelective synthesis of heterometallic systems and molecular rectangles have been developed.¹ These strategies include (i) the use of heteroditopic ligands with distinct coordination sites that recognize and selectively bind different metal ions,³ (ii) protection/deprotection routes starting from homoditopic ligands,⁴ and (iii) sequential two-step syntheses via (kinetically inert) mononuclear corner complexes, the so-called “Coupe du Roi” strategy.⁵

Some pyrazolate (pz)-based compartmental ligands⁶ have proven to be well-suited for the assembly of grid complexes.^{7,8} Using the rigid bis(tridentate) pyrazole ligand HL (HL = 3,5-bis(bipyridyl)pyrazole; Scheme 1), we recently reported a novel type of $[2 \times 2]$ Fe_4 grid complex that exhibits unprecedented multistability with respect to spin crossover and redox switching.⁷ In some experiments aimed at oxidizing the $[LFe^{II}_4]^{4+}$ grid to the mixed-valent $[L_4Fe^{II}_2Fe^{III}_2]^{6+}$ species, we now observed, as a minor side product, the formation of an unusual heterometallic $[L_4Fe^{III}_2(Ag_2)_2]^{6+}$ complex. It appears that partial grid degradation and replacement of some Fe^{II} by Ag^I , concomitant with oxidation of the remaining Fe, had occurred in that reaction. In this Communication, we present a targeted high-yield synthesis and full characterization of the unique hexametallc Fe^{III}/Ag^I complex. While Ag^I ions have been used to assemble discrete $[2 \times 2]$ Fe_4 complexes bearing peripheral N-donor groups into 1D and 2D superstructures,⁹ this appears to be the first report of a system containing both Ag and Fe *within* a gridlike motif.

Scheme 1. Ligand HL and Schematic Illustration of the One-Pot Synthesis of **2** via the Intermediate Corner Complex **1**^a



^aBlack bar: ligand molecule. Red balls: Fe^{II} . Blue balls: Fe^{III} . Gray balls: Ag^I .

The controlled synthesis of $[L_4Fe^{III}_2(Ag_2)_2]^{6+}$ is best carried out as a one-pot reaction. In a first step, the ligand HL and 0.5 equiv of $Fe(BF_4)_2$ are combined to give the “corner complex” $[Fe^{II}(HL)_2](BF_4)_2$ (**1**) as a key intermediate. **1** has been isolated and characterized by X-ray diffraction. Its solid-state structure reveals that this compound forms dimers that are held together by four $N^{Pz}-H \cdots N^{Py}$ (py = pyridine) hydrogen bonds (Figure 1). Hence, **1** is best described as $[Fe^{II}(HL)_2](BF_4)_4$,

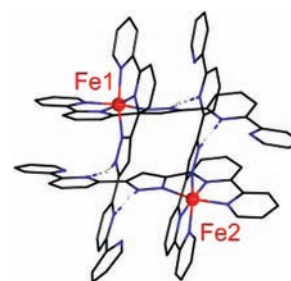


Figure 1. Molecular structure of the hydrogen-bonded dimer $\{[Fe(HL)_2]^{2+}\}_2$ of **1**. Solvent molecules and counterions are omitted for clarity.

which essentially is a $[2 \times 2]$ grid devoid of the metal ions at two opposite corners of the square. The 80 K Mössbauer spectrum confirms the low-spin ferrous nature of **1** ($\delta = 0.32$ mm s^{-1} and $\Delta E_Q = 0.88$ mm s^{-1} ; Figure S1 in the Supporting Information, SI). $N^{Pz} \cdots N^{Py}$ distances of 2.90–2.99 Å (Table S4

Received: March 15, 2012

Published: April 24, 2012



in the SI) indicate the presence of hydrogen bonds at the metal-free vertices.¹⁰ Thus, **1** appears to be well-preorganized for inserting additional metal ions at the two empty vertices to complete a regular metallosquare. This again underlines the high tendency of HL to form $[2 \times 2]$ grid structures. Electrospray ionization mass spectrometry spectra of MeCN solutions of **1**, however, do only show signals characteristic for the mononuclear species $[\text{Fe}(\text{H}_x\text{L})_2]^{y+}$ ($x = 0, 1$ and $y = 1, 2$; see Figure S3 in the SI), suggesting that the gridlike arrangement observed in the solid state largely dissociates when dissolved (at least in polar solvents such as MeCN).

Treatment of a solution of **1** in nitromethane with an excess of AgBF_4 and the subsequent addition of Na_2CO_3 lead to oxidation of the Fe^{II} ions and ligand deprotonation and eventually to the incorporation of Ag^+ to give the target product $[\text{L}_4\text{Fe}^{\text{III}}_2(\text{Ag}^{\text{I}}_2)_2](\text{BF}_4)_6$ (**2**). Thin blue crystal plates suitable for X-ray diffraction were grown by the slow diffusion of diethyl ether into a solution of **2** in nitromethane.

The molecular structure of the hexametallc Fe_2Ag_4 complex **2** has been determined by X-ray crystallography. In **2**, the roughly parallel arrangement of pairs of ligands is retained, but the protons found at two corners of **1** have been replaced by Ag^+ and the grid is distorted to a rhomboid. Thus, the $\{\text{N}_6\}$ pockets at those opposite corners of the rhomboid each host a Ag^{I}_2 dumbbell with a remarkably short $\text{Ag}-\text{Ag}$ distance (2.93 Å for $\text{Ag}1-\text{Ag}2$ and 2.88 Å for $\text{Ag}3-\text{Ag}4$), which is indicative of $d^{10}-d^{10}$ interactions.¹¹ $\text{Ag}-\text{N}$ distances range from 2.134 Å ($\text{Ag}-\text{N}^{\text{pz}}$) to 2.914 Å. When the $\text{Ag}-\text{Ag}$ interaction is neglected, the coordination environment of the Ag^+ ions is best described as $\{3 + 1\}$: three N donors are arranged almost in a plane, and one of them (a pyridine N) forms a weak asymmetric bridge to the apical position of a neighboring Ag^+ . Additionally, on the backsides, the Ag^+ ions appear to be stabilized by close contacts (3.12 and 2.99 Å) with the π system of a proximate bipyridine unit that is bound to Fe^{III} . These distances are above the usual $\text{Ag}-\pi$ interactions¹² but below the sum of the van der Waals radii.¹³

The two Fe^{III} ions located at the other two vertices of the rhomboid are crystallographically distinct, although their coordination environment is very similar. Their $\{\text{N}_6\}$ donor sets originate from two ligand strands, and the coordination sphere is strongly distorted from octahedral (some angles deviate up to 11% from the ideal octahedral angles). The average $\text{Fe}-\text{N}$ bond length is 1.94 Å; bonds involving the terminal pyridine N atoms are, however, slightly longer (average 1.99 Å). Overall, the six metal ions in **2** form an almost perfectly planar hexagon (maximum out-of-plane deviation 0.2 Å; Figure 2) with two short $\text{Ag}-\text{Ag}$ edges.

The Mössbauer spectrum of a crystalline sample of **2** at 80 K features an unsymmetric doublet (Figure 3, left); this signature is largely independent of the temperature (see Figure S2). Experimental data have been fitted by assuming two subspectra with slightly different isomer shifts ($\delta_1 = 0.16 \text{ mm s}^{-1}$ and $\delta_2 = 0.05 \text{ mm s}^{-1}$) and quadrupole splittings ($\Delta E_{\text{Q},1} = 3.04 \text{ mm s}^{-1}$ and $\Delta E_{\text{Q},2} = 3.25 \text{ mm s}^{-1}$), both typical for low-spin Fe^{III} . Observing two subspectra for the solid material may be rationalized in view of the presence of two crystallographically distinct Fe^{III} vertices in the crystal structure.¹⁴ Unexpectedly, however, the Mössbauer spectrum of a solution of **2** in MeNO_2 (10 mM) looks very much alike and again requires the assumption of two subspectra for proper fitting of the experimental data ($\delta_1 = 0.12 \text{ mm s}^{-1}$ and $\delta_2 = 0.05 \text{ mm s}^{-1}$; $\Delta E_{\text{Q},1} = 3.15 \text{ mm s}^{-1}$ and $\Delta E_{\text{Q},2} = 3.26 \text{ mm s}^{-1}$; Figure 3,

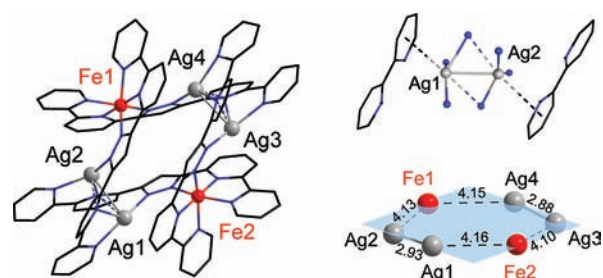


Figure 2. Left: Molecular structure of **2**, determined by X-ray diffraction at 133 K. Solvent molecules and counterions are omitted for clarity. Top right: Coordination environment of the Ag_2 units. Dashed blue line: $\text{Ag}-\text{N}$ distances above 2.7 Å. Bottom right: Hexagon of metal ions in **2**.

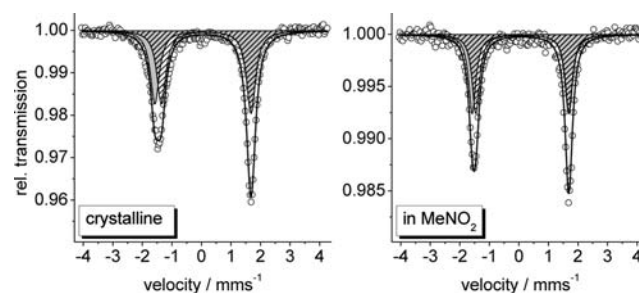


Figure 3. Mössbauer spectra recorded at 80 K for a crystalline sample (left) and a frozen solution sample (MeNO_2 , 10 mM). Subpectrum 1: gray color. Subpectrum 2: patterned.

right). The reason for the nonequivalence of the two Fe^{III} ions in solution remains unclear.

A SQUID measurement of solid **2** confirms the presence of two magnetically uncoupled low-spin Fe^{III} ions: χT is largely independent of the temperature and matches the spin-only value expected for two uncoupled $S = 1/2$ sites (with $g = 2.10$; see Figure S2 in the SI). The electronic spectrum of a solution of **2** in a nitromethane solution (380–1500 nm, Figure 4)

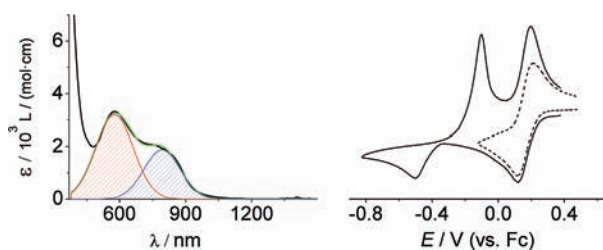


Figure 4. Left: Electronic absorption spectrum of a solution of **2** in MeNO_2 (0.1 mmol L^{-1}). Right: Cyclic voltammogram of a solution of **2** in $\text{MeCN}/0.1 \text{ M } n\text{Bu}_4\text{NPF}_6$ at a scan rate of 100 mV s^{-1} .

reveals very strong bands in the UV region ($<400 \text{ nm}$) due to ligand-based $\pi \rightarrow \pi^*$ transitions. Additional low-energy absorptions at 800 nm ($\epsilon = 1900 \text{ L mol}^{-1} \text{ cm}^{-1}$) and 580 nm ($\epsilon = 3200 \text{ L mol}^{-1} \text{ cm}^{-1}$) are tentatively assigned to ligand-to-metal charge-transfer transitions involving the Fe^{III} ions. The spectrum of **2** closely resembles the spectrum of the related mixed-valent grid complex $[\text{L}_4\text{Fe}^{\text{III}}_2\text{Fe}^{\text{II}}_2]^{6+}$ ($\lambda_{\text{max}} = 587$ and 749 nm),⁷ which supports the idea that these two absorptions originate from the Fe^{III} chromophore. Cyclic voltammetry of **2** in a MeCN solution reveals a reversible reduction process at relatively high potential ($E_{1/2} = +0.165 \text{ V}$; Figure 4), which

likely represents the $\text{Fe}^{\text{III}}/\text{Fe}^{\text{II}}$ pair. This implies that the two ferric ions at two opposite vertices are electronically largely uncoupled, as expected. A further reduction process at more negative potential is irreversible ($E_{\text{p}}^{\text{red}} = -0.50$ V) and most likely corresponds to the reduction of Ag^{I} . An anodic wave in the backscan (at $E_{\text{p}}^{\text{ox}} = -0.10$ V) might be caused by Ag stripping from the electrode.

While a few $[2 \times 2]$ Ag_4 square complexes have been reported,¹⁵ the presence of dumbbell-like Ag_2 vertices in **2** appears to be unprecedented for grid-type systems. Also, the combination of Ag^{I} and Fe in discrete oligonuclear complexes is quite rare because such compounds usually contain Fe^{II} ,¹⁶ in contrast to the heterometallic $\text{Ag}^{\text{I}}/\text{Fe}^{\text{III}}$ complex **2**. In conclusion, the $[2 \times 2]$ grid $[\text{LFe}^{\text{II}}_4]^{4+}$, although quite robust, upon oxidation with Ag^{I} may loose some of its Fe and transform to an unusual and expanded rhombiclike structure with Ag_2 dumbbells at two opposite vertices. This hexametallic $[\text{L}_4\text{Fe}^{\text{III}}_2(\text{Ag}_2)_2]^{6+}$ complex has now been prepared selectively and fully characterized. The complete exchange of all four Fe vertices in $[\text{LFe}^{\text{II}}_4]^{4+}$ by Ag_2 dumbbells to give an $[\text{L}(\text{Ag}_2)_4]^{4+}$ gridlike system appears to be an attractive perspective.

■ ASSOCIATED CONTENT

📄 Supporting Information

X-ray crystallographic data in CIF format, experimental details, Mössbauer data for **1** and **2**, χT versus T data for **2**, crystallographic data with bond lengths and angles. This material is available free of charge via the Internet at <http://pubs.acs.org>.

■ AUTHOR INFORMATION

Corresponding Author

*E-mail: franc.meyer@chemie.uni-goettingen.de.

Author Contributions

All authors have given approval to the final version of the manuscript.

Notes

The authors declare no competing financial interest.

■ ACKNOWLEDGMENTS

Financial support by the Deutsche Forschungsgemeinschaft (SFB 602, Project A16) is gratefully acknowledged. We thank Jörg Teichgräber for the cyclic voltammetry measurement.

■ REFERENCES

- (1) (a) Ruben, M.; Rojo, J.; Romero-Salguero, F. J.; Uppadine, L. H.; Lehn, J.-M. *Angew. Chem., Int. Ed.* **2004**, *43*, 3644–3662. (b) Dawe, L. N.; Abedin, T. S. M.; Thompson, L. K. *Dalton Trans.* **2008**, 1661–1675. (c) Dawe, L. N.; Shuvaev, K. V.; Thompson, L. K. *Chem. Soc. Rev.* **2009**, *38*, 2334–2359.
- (2) Ruben, M.; Lehn, J.-M.; Müller, P. *Chem. Soc. Rev.* **2006**, *35*, 1056–1067.
- (3) Uppadine, L. H.; Gisselbrecht, J.; Kyritsakas, N.; Näntinen, K.; Rissanen, K.; Lehn, J.-M. *Chem.—Eur. J.* **2005**, *11*, 2549–2565.
- (4) Bassani, D. M.; Lehn, J.-M.; Fromm, K.; Fenske, D. *Angew. Chem., Int. Ed.* **1998**, *37*, 2364–2367.
- (5) Uppadine, L. H.; Lehn, J.-M. *Angew. Chem., Int. Ed.* **2004**, *43*, 240–243.
- (6) Klingele, J.; Dechert, S.; Meyer, F. *Coord. Chem. Rev.* **2009**, *253*, 2698–2741.
- (7) Schneider, B.; Demeshko, S.; Dechert, S.; Meyer, F. *Angew. Chem., Int. Ed.* **2010**, *49*, 9274–9277.
- (8) (a) Zhang, H.; Fu, D.; Ji, F.; Wang, G.; Yu, K.; Yao, T. *J. Chem. Soc., Dalton Trans.* **1996**, 3799–3803. (b) Mann, K. L. V.; Psillakis, E.;

Jeffery, J. C.; Rees, L. H.; Harden, N. M.; McCleverty, J. A.; Ward, M. D.; Gatteschi, D.; Totti, F.; Mabbs, F. E.; McInnes, E. J. L.; Riedi, P. C.; Smith, G. M. *J. Chem. Soc., Dalton Trans.* **1999**, 339–348. (c) van der Vlugt, J. I.; Demeshko, S.; Dechert, S.; Meyer, F. *Inorg. Chem.* **2008**, *47*, 1576–1585. (d) Klingele, J.; Prikhod'ko, A. I.; Leibel, G.; Demeshko, S.; Dechert, S.; Meyer, F. *Dalton Trans.* **2007**, 2003–2013. (e) Matsumoto, T.; Shiga, T.; Noguchi, M.; Onuki, T.; Newton, G. N.; Hoshino, N.; Nakano, M.; Oshio, H. *Inorg. Chem.* **2010**, *49*, 368–370.

(9) Ruben, M.; Ziener, U.; Lehn, J.-M.; Ksenofontov, V.; Gülich, P.; Vaughan, G. B. M. *Chem.—Eur. J.* **2005**, *11*, 94–100.

(10) Both Mössbauer spectroscopy and X-ray crystallography indicate that minor amounts of gridlike species with three or even four Fe^{II} are present in crystalline samples of **1**, even after repeated recrystallization (see the SI).

(11) Schmidbaur, H.; Schier, A. *Chem. Soc. Rev.* **2008**, *37*, 1931–1951.

(12) (a) Khlobystov, A. N.; Blake, A. J.; Champness, N. R.; Lemenovskii, D. A.; Majouga, A. G.; Zyk, N. V.; Schröder, M. *Coord. Chem. Rev.* **2001**, *222*, 155–192. (b) Mascá, M.; Kerdelhué, J.; Blake, A. J.; Cooke, P. A.; Mortimer, R. J.; Teat, S. J. *Eur. J. Inorg. Chem.* **2000**, 485–490.

(13) Bondi, A. J. *Phys. Chem.* **1964**, *68*, 441–451.

(14) The line shape is largely independent of the temperature, which argues against relaxation effects as a cause for the asymmetry.

(15) (a) Schottel, B. L.; Chifotides, H. T.; Shatruk, M.; Chouai, A.; Perez, L. M.; Basca, J.; Dunbar, K. R. *J. Am. Chem. Soc.* **2006**, *128*, 5895. (b) Price, J. R.; Lan, Y.; Jameson, G. B.; Brooker, S. *Dalton Trans.* **2006**, 1491. (c) Price, J. R.; White, N. G.; Perez-Velasco, A.; Jameson, G. B.; Hunter, C. A.; Brooker, S. *Inorg. Chem.* **2008**, *47*, 10729. (d) Constable, E. C.; Zhang, G.; Housecroft, C. E.; Zampese, J. A. *CrystEngComm* **2010**, *12*, 3724.

(16) Piguet, C.; Bernardinelli, G.; Williams, A. F.; Bocquet, B. *Angew. Chem., Int. Ed.* **1995**, *34*, 582–584.